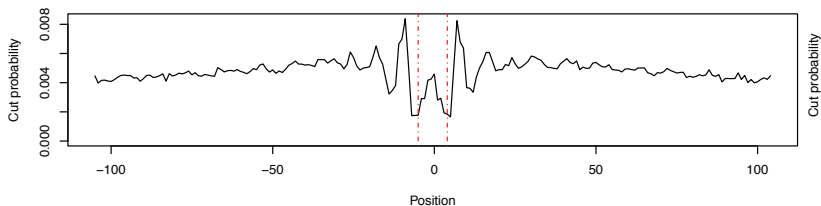


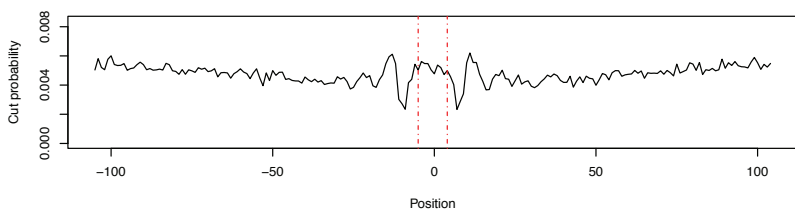
Figure S1: Aggregate footprint profiles for FOXO1, MEF2D, CEBPA, and CREB3I2 in adipose tissue samples. Footprints are shown for adipose tissue sample 1; results were similar for tissue samples 2 and 3. Bound, unbound, and normalized profiles are shown for each factor.

NFIA

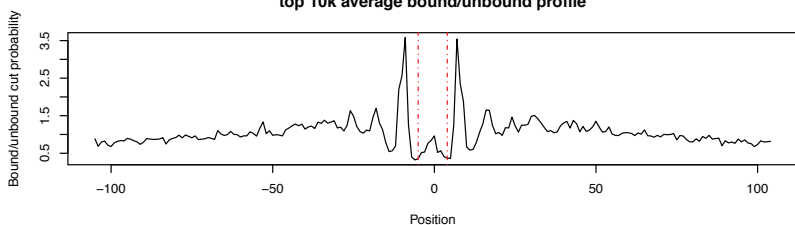
Average profile at bound sites



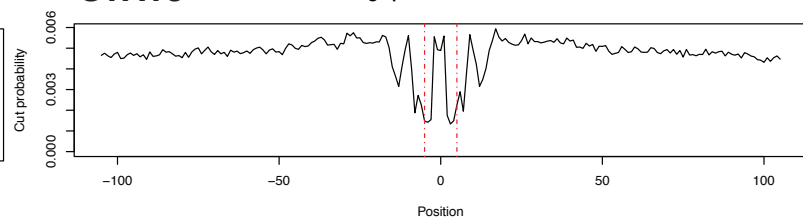
Average profile at unbound sites



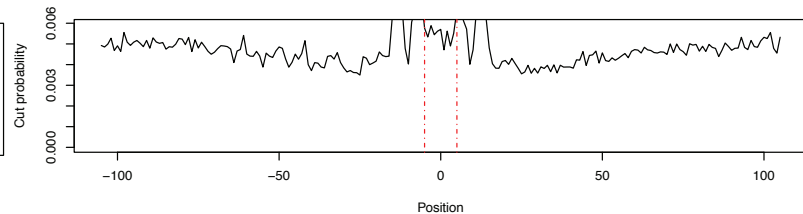
top 10k average bound/unbound profile

**STAT3**

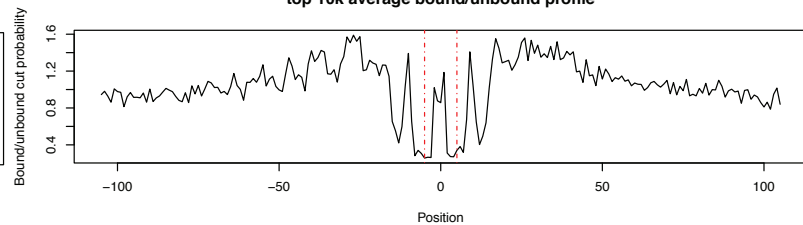
Average profile at bound sites



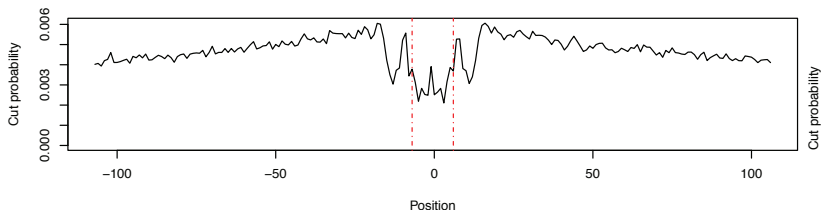
Average profile at unbound sites



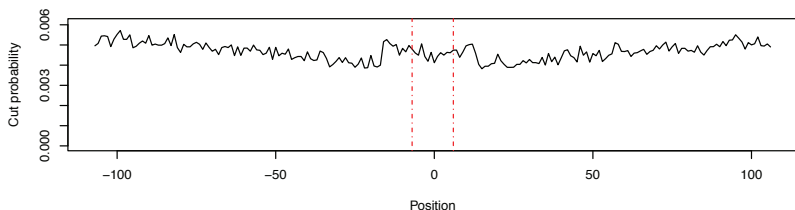
top 10k average bound/unbound profile

**SPI1**

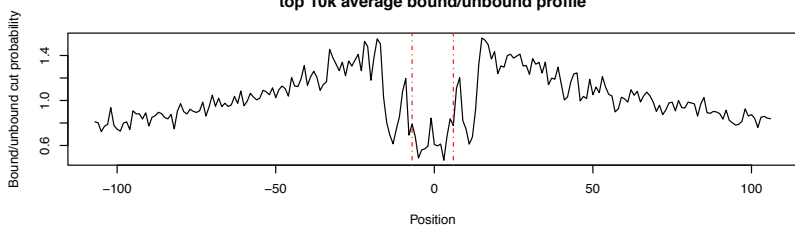
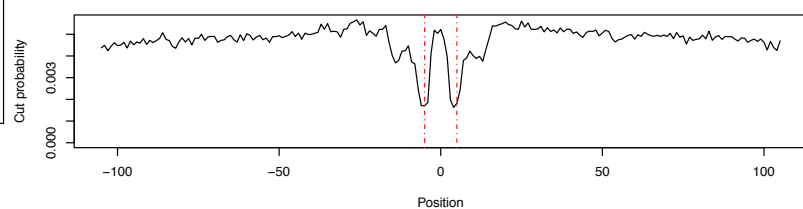
Average profile at bound sites



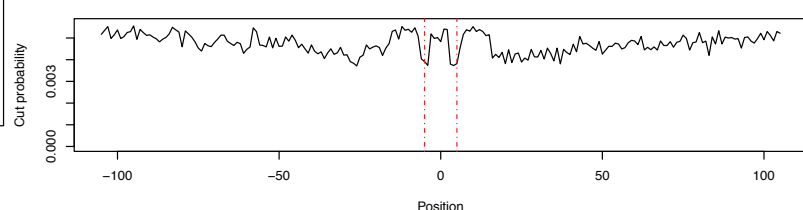
Average profile at unbound sites



top 10k average bound/unbound profile

**STAT5A::STAT5B** Average profile at bound sites

Average profile at unbound sites



top 10k average bound/unbound profile

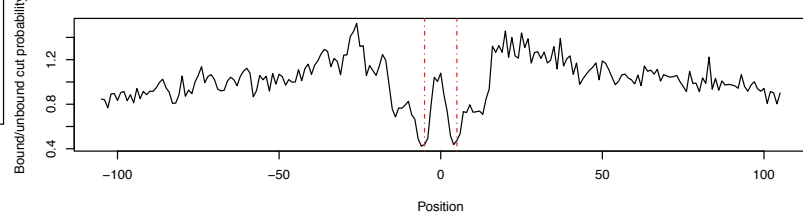


Figure S2: Aggregate footprint profiles for NFIA, SPI1, STAT3, and STAT5A::STAT5B in adipose tissue samples. Footprints are shown for adipose tissue sample 1; results were similar for tissue samples 2 and 3. Bound, unbound, and normalized profiles are shown for each factor.

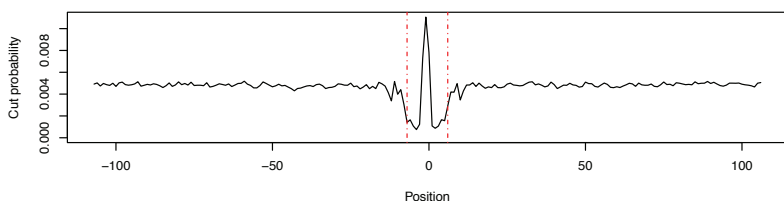
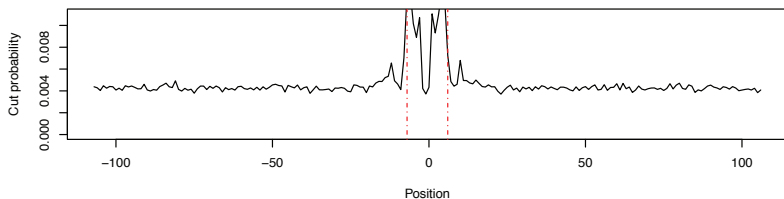
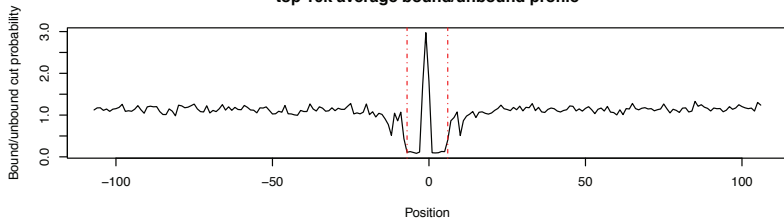
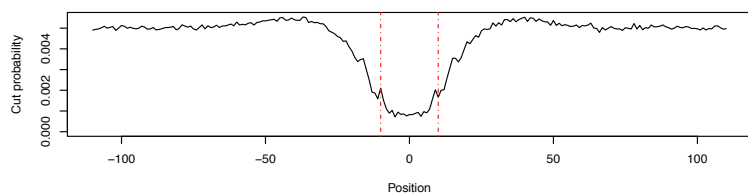
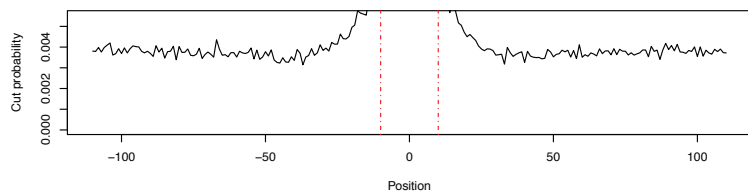
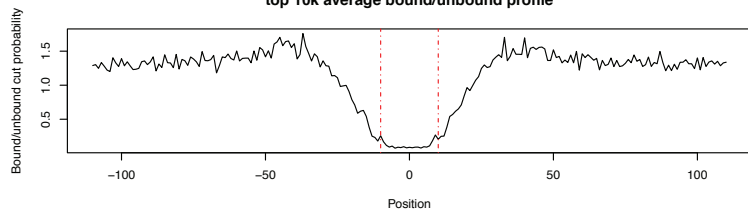
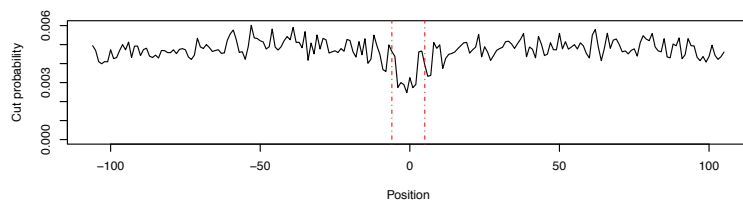
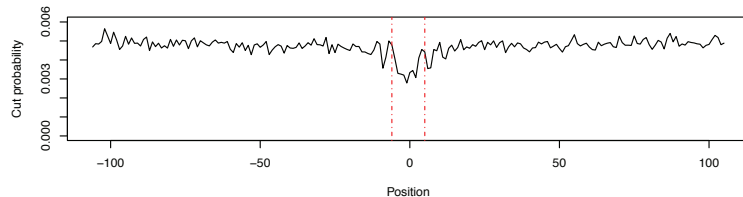
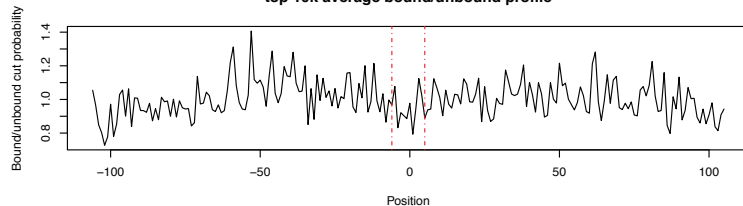
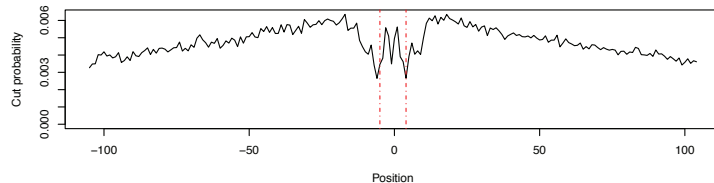
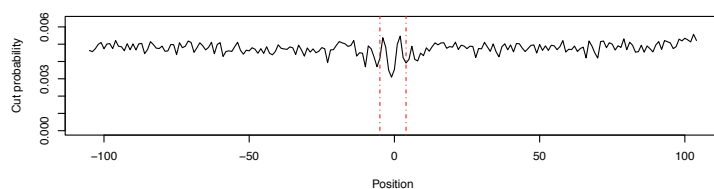
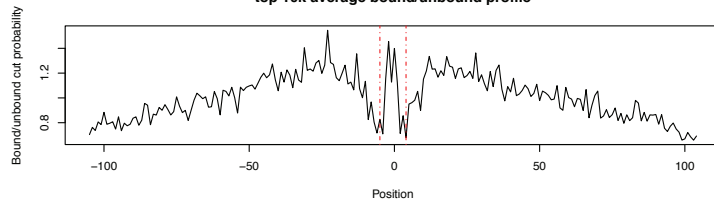
TCF7L2**Average profile at bound sites****Average profile at unbound sites****top 10k average bound/unbound profile****IRF1****Average profile at bound sites****Average profile at unbound sites****top 10k average bound/unbound profile****PBX1****Average profile at bound sites****Average profile at unbound sites****top 10k average bound/unbound profile****ETS1****Average profile at bound sites****Average profile at unbound sites****top 10k average bound/unbound profile**

Figure S3: Aggregate footprints for TCFL7, IRF1, PBX1, and ETS1. Aggregate footprints for TCFL7 were observed in all three adipose tissue samples. An aggregate footprint for IRF1 was observed in adipose samples 1 and 3; PBX1 in adipose samples 1 and 2; and ETS1 in adipose sample 2. For footprints in more than one sample, profiles are shown for adipose sample 1. Bound, unbound, and normalized profiles are shown for each factor.

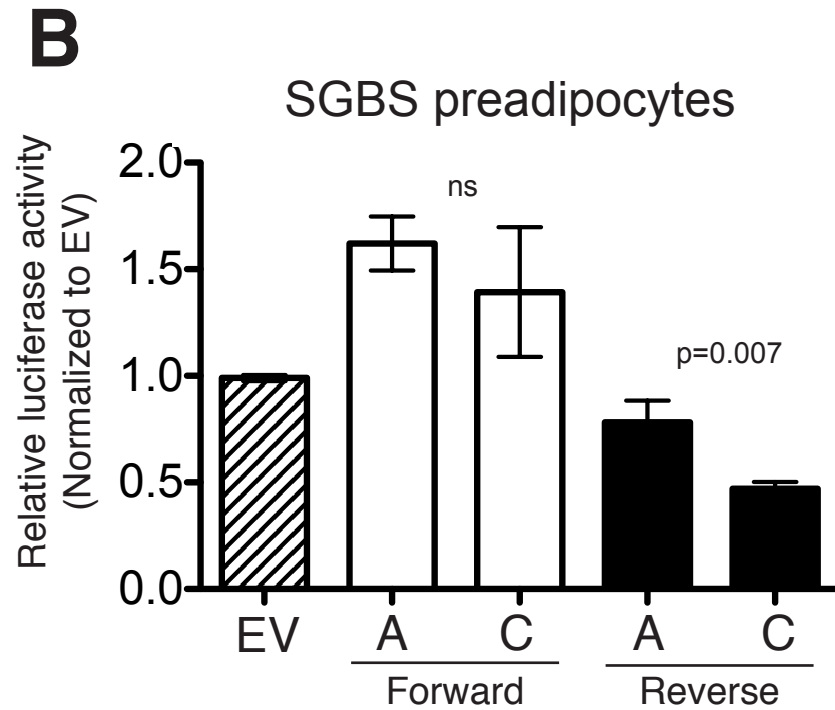
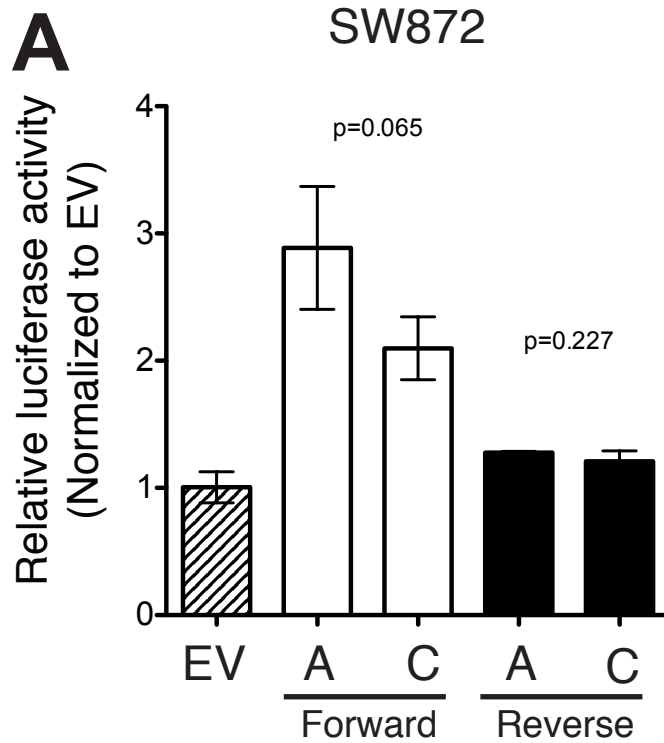


Figure S4. Additional regulatory assay for rs1534696. The region containing rs1534696 was tested in transcriptional reporter luciferase assays in SW872 (A) and SGBS preadipocyte (B) cells. Each bar represents mean \pm standard deviation of three independent clones. The trend of higher transcriptional activity for rs1534696-A is consistent with results in 3T3-L1 preadipocytes and adipocytes (Figure 4).

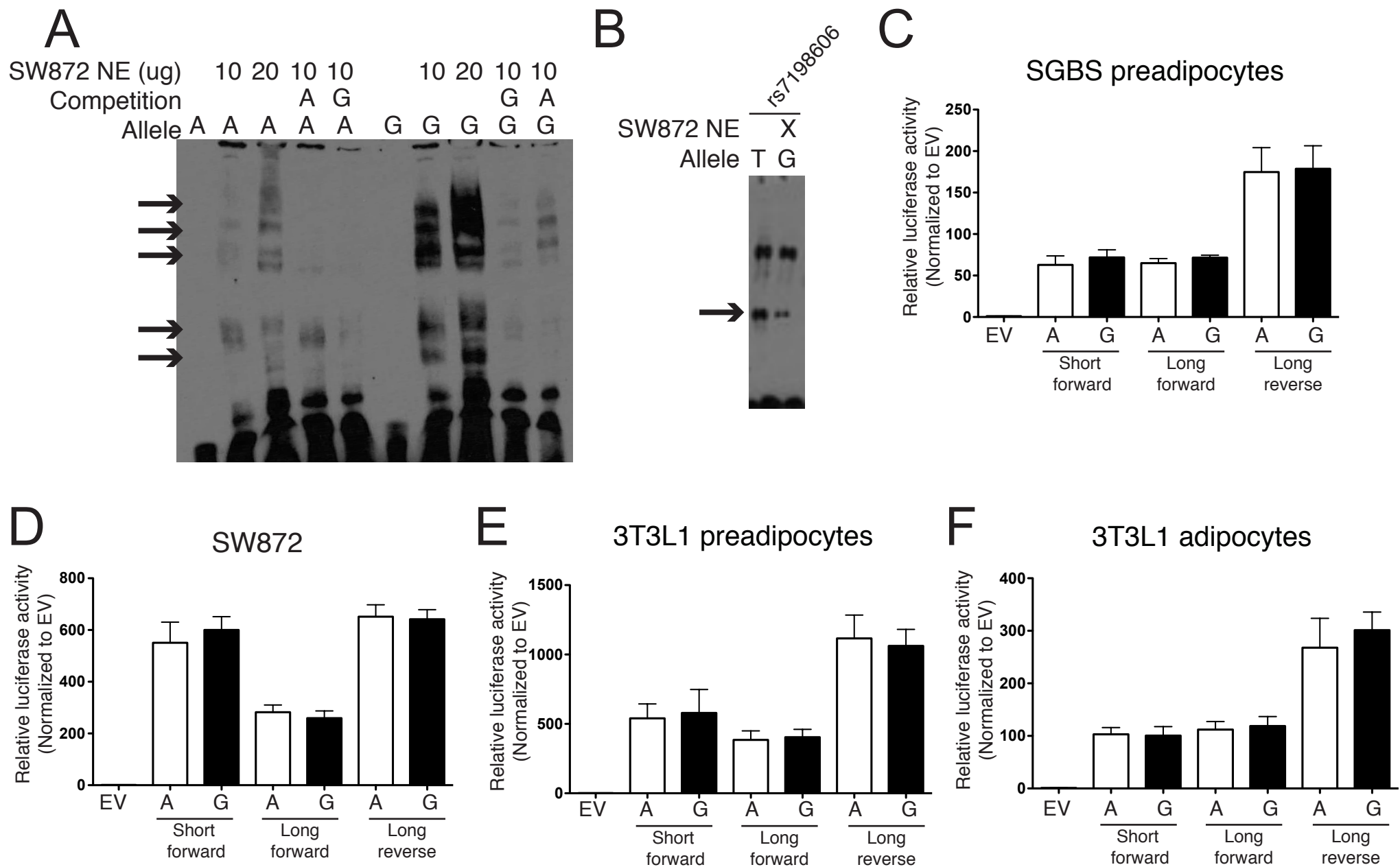


Figure S5. Additional regulatory assays for rs7187776. (A) rs7187776-G shows increased protein binding using SW872 nuclear extract in EMSA. The banding pattern of protein binding is similar to binding to purified PU.1 (Figure 5). Arrows indicate allelic differences. (B) One of four additional variants (rs7198606) overlapping ATAC-seq peaks show allelic differences in protein binding (arrow) using SW872 nuclear extract in EMSA. The remaining three variants did not show consistent results across EMSA experiments. (C-F) The region containing rs7187776 shows extremely strong transcriptional activity in reporter assays in (C) SGBS preadipocytes, (D) SW872 cells, (E) 3T3L1 preadipocytes, (F) 3T3L1 adipocytes. There were no significant allelic differences. Bars represent the mean \pm standard deviation of 3-5 independent clones.